

Supporting Information

Decamethylcucurbit[5]uril based Supramolecular Assemblies as Efficient Electrocatalysts for Oxygen Reduction Reaction

Ruru Chen,^{ab} Minna Cao,^{*,a} Jinyun Wang,^a Hongfang Li,^a and
Rong Cao^{*,a}

a. State Key Laboratory of Structural Chemistry, Fujian Institute
of Research on the Structure of Matter, Chinese Academy of
Sciences, Fuzhou 350002, China.

b. College of Chemistry, Fuzhou University, Fuzhou 350108,
China.

Corresponding Authors

*Minna Cao (mncao@fjirsm.ac.cn); *Rong Cao (rcao@fjirsm.ac.cn)

Experimental:

1.1 Materials

Alkali metal chloride (MCl, M = Na, K, Rb, Cs) and perchloric acid (HClO₄) were bought from Sinopharm Chemical Reagent. Nafion solution (5 wt%) was purchased from Sigma-Aldrich. Chloroplatinic acid hydrate (H₂PtCl₆•6H₂O) (99.9%) was bought from J&K Chemical Reagent. Commercial Pt/C was bought from Alfa. All chemicals were used directly without further purification. Me₁₀CB[5] was synthesized according to the process reported in the literature.¹ Ultrapure water (18 MΩ) used in the experiments was supplied by a Millipore System.

1.2 Synthesis of MPtMe₁₀CB[5] (M = Na, K, Rb, Cs) supramolecular assembly.

The Pt precursors were firstly assembled with Me₁₀CB[5] in the presence of various alkali metal ions (Na⁺, K⁺, Rb⁺, and Cs⁺) to produce a series of supramolecular assemblies MPtMe₁₀CB[5] (M = Na, K, Rb, Cs). In a typical synthetic process, 88 mg (0.17 mmol) of H₂PtCl₆•6H₂O was dissolved in 20 mL of ultrapure water to obtain a clear aqueous solution of H₂PtCl₆ (solution I). Me₁₀CB[5] (100 mg, 0.1 mmol) and alkali metal chloride (0.2 mmol) were dissolved into the ultrapure water (20 mL) under ultrasonic (solution II). Solutions I and II were carefully transferred to each side of an H-tube, respectively. Orange crystals were obtained after three days in the H-tube by slow diffusion. Combined with elemental analyses (EA) and thermogravimetric analysis (TGA) results, the formulas of the supramolecular assemblies have been confirmed.

[Na₂(Me₁₀CB[5]@H₂O)][PtCl₆]•5H₂O (1): elemental analysis calcd (%) for C₄₀H₆₂N₂₀O₁₆Cl₆Na₂Pt, C, 30.96%; H, 4.13%; N, 18.06%; Found: C, 31.11%; H, 4.18%, N, 18.91%.

[K₂(Me₁₀CB[5]@H₂O)][PtCl₆]•3H₂O (2): elemental analysis calcd (%) for C₄₀H₅₈N₂₀O₁₄Cl₆K₂Pt, C, 31.39%; H, 3.79%; N, 18.31%; Found: C, 31.90%; H, 3.61%; N, 18.36%.

[Rb₂(Me₁₀CB[5]@H₂O)][PtCl₆]•H₂O (3): elemental analysis calcd (%) for C₄₀H₅₄N₂₀O₁₂Cl₆Rb₂Pt: C: 30.26%; H: 3.40%; N: 17.65%; Found: C, 29.90%; H, 3.12%; N, 17.25%.

[Cs₂(Me₁₀CB[5]@H₂O)][PtCl₆]•H₂O (4): elemental analysis calcd (%) for C₄₀H₅₄N₂₀O₁₂Cs₂Pt, C, 28.56%; H, 3.21%; N, 16.66%; Found: C, 28.83%; H, 3.05%; N, 16.53%.

1.3 Characterization:

Transmission electron microscope (TEM) and high-angle annular dark-field scanning transmission electron microscopy (HAADF-STEM) were performed on a FEI Tecnai G2 F20 electron microscope at 200 kV. X-ray photoelectron spectroscopy (XPS) measurements were performed by an ESCALAB 250 Xi XPS system. Elemental analysis (EA) was carried on an Elementar Vario EL III analyzer. Powder X-ray diffraction (PXPD) patterns were performed with a Rigaku Miniflex 600 diffractometer with a Cu/K α radiation source ($\lambda = 1.5418 \text{ \AA}$) at a low scanning speed of 1°min^{-1} . Thermogravimetric analysis (TGA) was performed under a flow of nitrogen at a heating rate of $10^\circ\text{C min}^{-1}$, by using a TA SDT-Q600 instrument. Metal analysis was determined by using an inductively coupled plasma emission spectrometer (ICP) JobinYvonUltima 2. Single-crystal X-ray diffraction data were collected on a SuperNova CCD diffractometer equipped with graphite monochromatized Cu/K α radiation ($\lambda = 1.5418 \text{ \AA}$) (compound 1-3), Mo/K α radiation ($\lambda = 0.71073 \text{ \AA}$) (compound 4) with a CCD detector. Empirical absorption corrections were applied to the data using the Crystal Clear program.² Structures were solved by direct methods and refined on F^2 by full-matrix least-squares with the SHELXTL-2015 program package.³ All non-hydrogen atoms, except some water oxygen atoms, were refined anisotropically. The hydrogen atoms of organic molecules were generated geometrically. Crystal data and structure refinement parameters are given in Table S1. 1920207, 1915754, 1920206, 1921936 contain the supplementary crystallographic data for this paper. These data can be obtained free of charge from The Cambridge Crystallographic Data Centre.

1.4 Oxygen reduction reaction (ORR) Measurements.

The as-synthesized supramolecular assembly (10 mg) was grinded to powder and mixed with Vulcan XC-72R carbon black (10 mg) uniformly. The homogeneous ink was prepared using mixture of 0.7 mL water, 0.3 mL isopropyl alcohol, 40 μL 5 wt% Nafion solution with adding the physical mixture of MPtMe₁₀CB[5] and Vulcan XC-72R carbon black followed by ultrasonic for 2 h. Then, 40 μL of the ink was uniformly loaded onto a freshly polished glassy carbon (GC) (0.196 cm²) electrode. In all measurements, the Pt loading amount of the catalyst was 20 μg .

All the electrochemical studies were carried out with a standard three electrodes system using an IM6ex (Zahner, Germany). The GC modified with catalyst, Pt wire (1 \times 1 cm²) and Ag/AgCl electrode saturated with KCl were worked as working electrode, counter electrode and reference electrode, respectively. All the potentials were converted to the reversible hydrogen electrode (RHE) by adding a value of (0.197 + 0.0591 \times pH) V. Before doping the ink, the working electrode was fully polished by alumina slurry (1.0 mm, 0.3 mm and 0.05 mm) in sequence.

For all the electrochemical measurements, an aqueous of 0.1 M HClO₄ was employed as the electrolyte. N₂ or O₂ was purged continuously for 30 min to achieve an O₂-free or O₂-saturated condition. The tested materials were activated through scanning cyclic voltammetry (CV) with the sweeping rate of 100 mV s⁻¹ until the adjacent curves have complete overlap. All the linear sweep voltammetry (LSV) examination were recorded at a sweeping rate of 10 mV s⁻¹ and rotating speed of 1600 rpm under O₂-saturated condition.

Rotating disk electrode (RDE) measurements were performed using the Koutecky-Levich equation. This equation was used to determine the number of electrons transfer number involved in oxygen reduction. Koutecky-Levich plots were analyzed at various electrode potentials. The slopes of their best linear fit lines were used to calculate the number of electrons transfer number based on the Koutecky-Levich equation:

$$1/J = 1/J_L + 1/J_K = 1/B\omega^{0.5} + 1/J_K$$

Where J_K and J_L were the kinetic- and diffusion-limiting current densities, respectively, and ω was the angular velocity. B was Levich slope that was given by $B = 0.20 nFC_0D_0^{2/3}\nu^{-1/6}$, $J_K = nFkC_0$

Here n was the number of electrons transfer in the reduction process of one O_2 molecule, F was the Faraday constant ($F = 96485$ C/mol), D_{O_2} was the diffusion coefficient of O_2 in 0.1 M $HClO_4$ ($D_{O_2} = 1.67 \times 10^{-5}$ cm²/s), ν was the kinematics viscosity for $HClO_4$ ($\nu = 0.01$ cm²/s) and C_{O_2} was concentration of O_2 in the solution ($C_{O_2} = 1.38 \times 10^{-6}$ mol/cm³). The constant of 0.2 was adopted when the rotation speed was expressed in rpm.

Rotating ring-disk electrode (RRDE) measurement

RRDE measurements were recorded with catalyst inks and electrodes prepared by the same method as for the RDE measurements. The disk electrode was scanned at a rate of 10 mV/s and the ring potential constant at 1.5 V vs. RHE. The hydrogen peroxide yield ($H_2O_2\%$) and the electron transfer number (n) were calculated with the following equations:

$$H_2O_2(\%) = 200 \times \frac{\frac{I_r}{N}}{I_d + \frac{I_r}{N}}$$

$$n = 4 \times \frac{I_d}{I_d + \frac{I_r}{N}}$$

Where I_d is disk current, I_r is ring current and $N = 0.4$ is the current collection efficiency of the Pt ring.

Theoretical Calculation Methodology. All the calculations were implemented by using Gaussian 09 program package.⁴ The initial model of these five complexes was extracted from the crystal structures solved by single-crystal X-ray diffraction analysis. The hybrid Becke three-parameter Lee–Yang–Parr (B3LYP) functional with dispersion correction (B3LYP-D3)⁵ was used to describe the exchange and correlation interaction. In these calculations, the LANL2DZ basis set modified with the electrostatic core potentials (ECPs) was

used to describe the Na, K, Rb, Cs, and Pt atoms,⁶ while other non-metal atoms of Cl, O, N, C and H were described by the all-electron basis set of 6-31G**. Then, Atomic dipole corrected Hirshfeld atomic charge (ADCH)⁷ for Pt atoms are analyzed by using Multiwfn 3.3 program.⁸

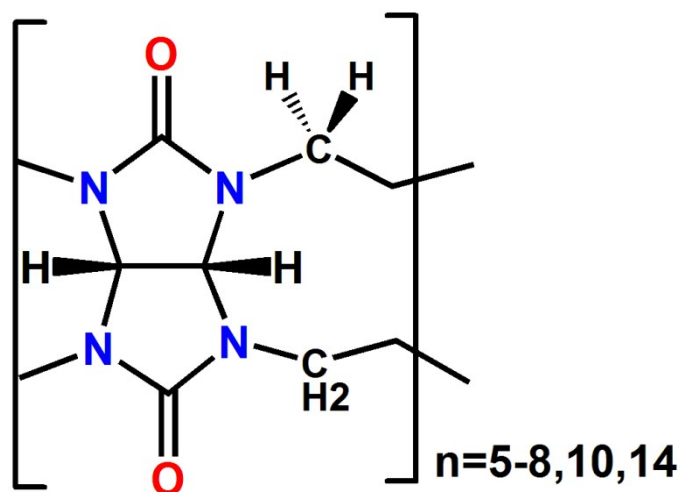


Fig. S1. Structural presentation of CB[n]s.

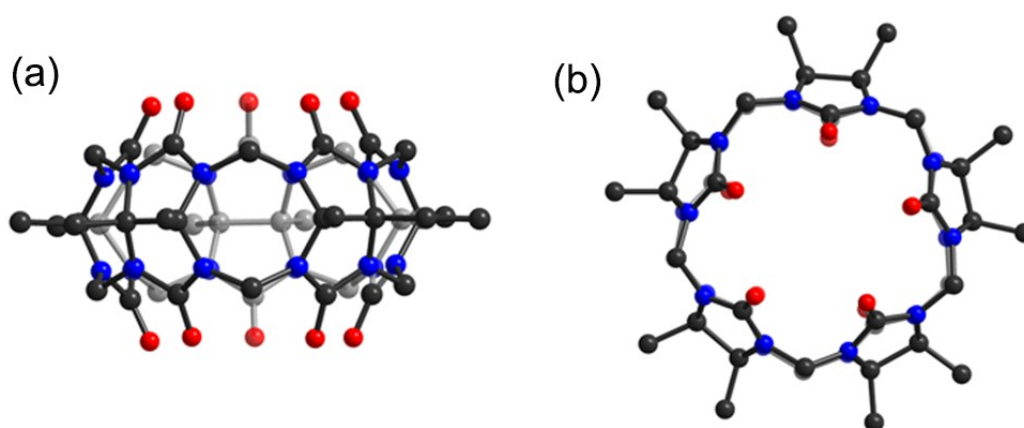


Fig. S2. Side and top views of Me₁₀CB[5], red is O atom, blue is N atom, black is C atom.

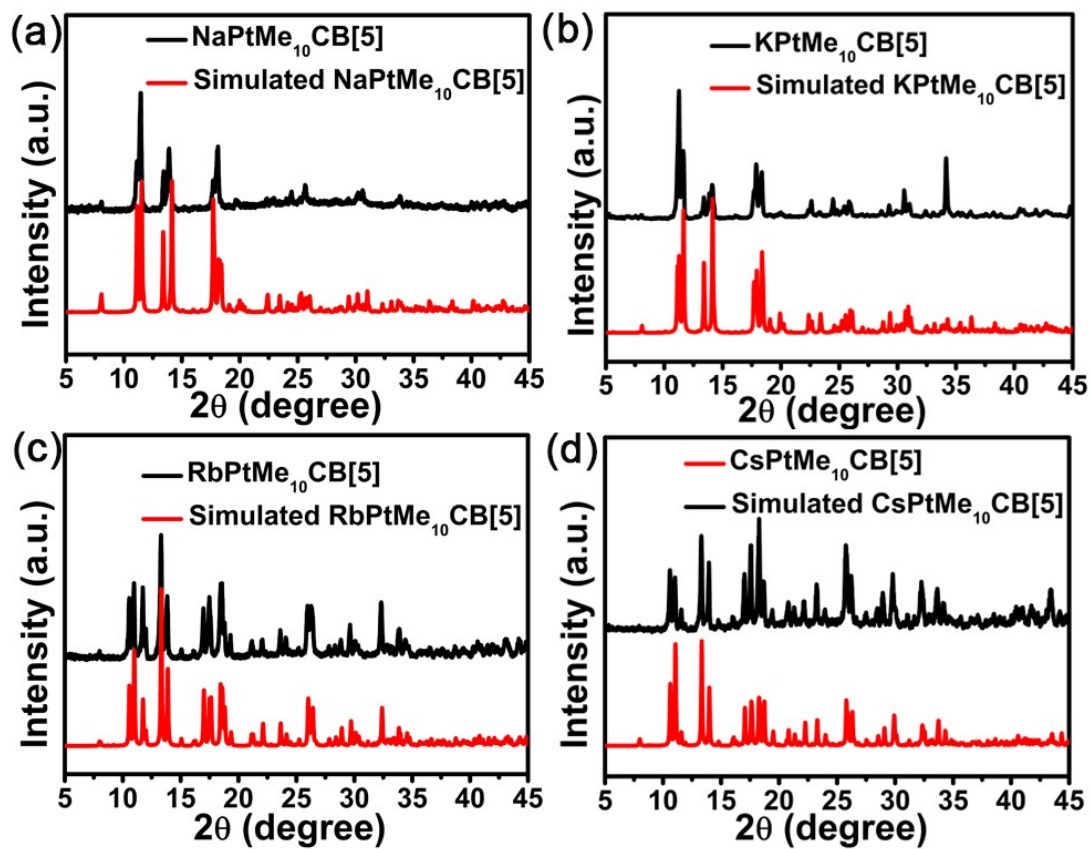


Fig. S3. PXRD patterns of (a) NaPtMe₁₀CB[5] (b) KPtMe₁₀CB[5] (c) RbPtMe₁₀CB[5] (d) CsPtMe₁₀CB[5]

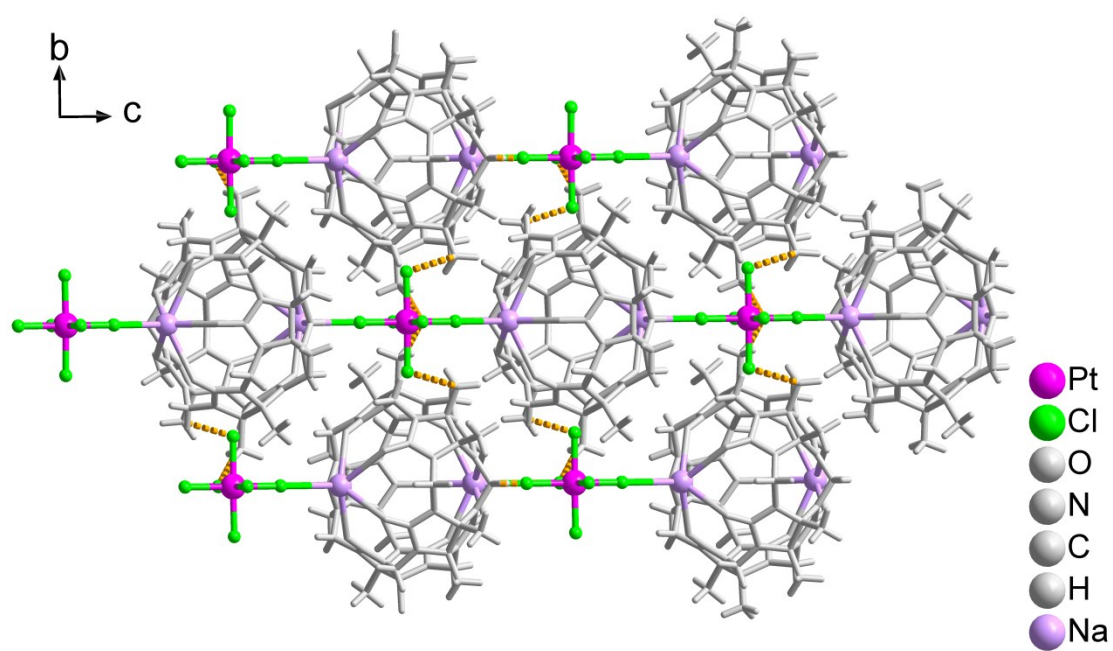


Fig. S4. The 3D images of NaPtMe₁₀CB[5].

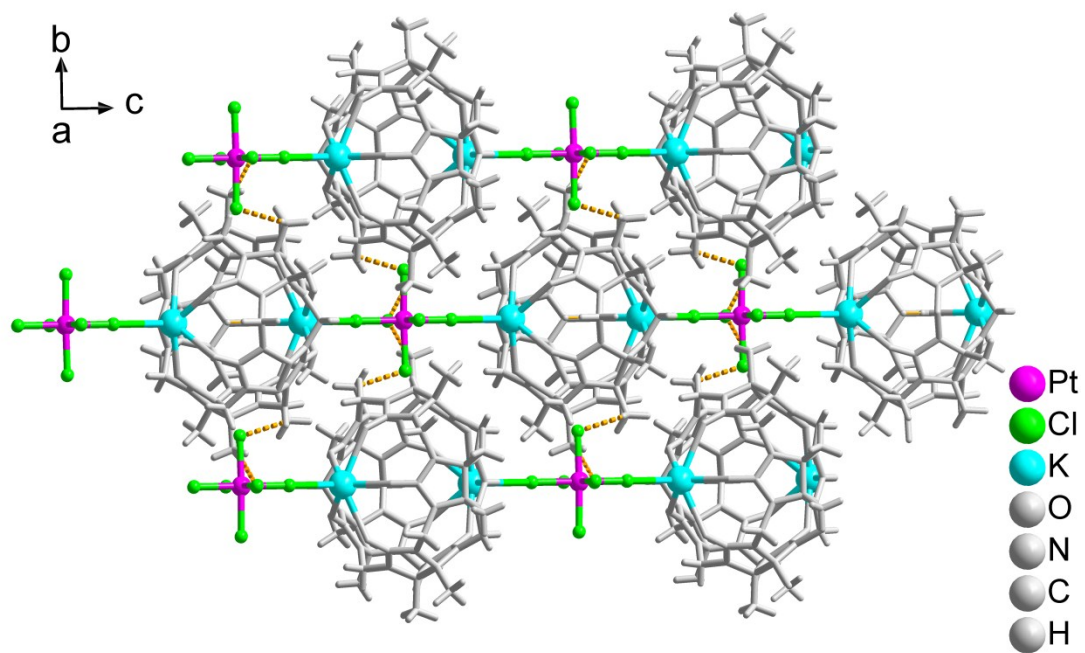


Fig. S5. The 3D images of KPtMe₁₀CB[5].

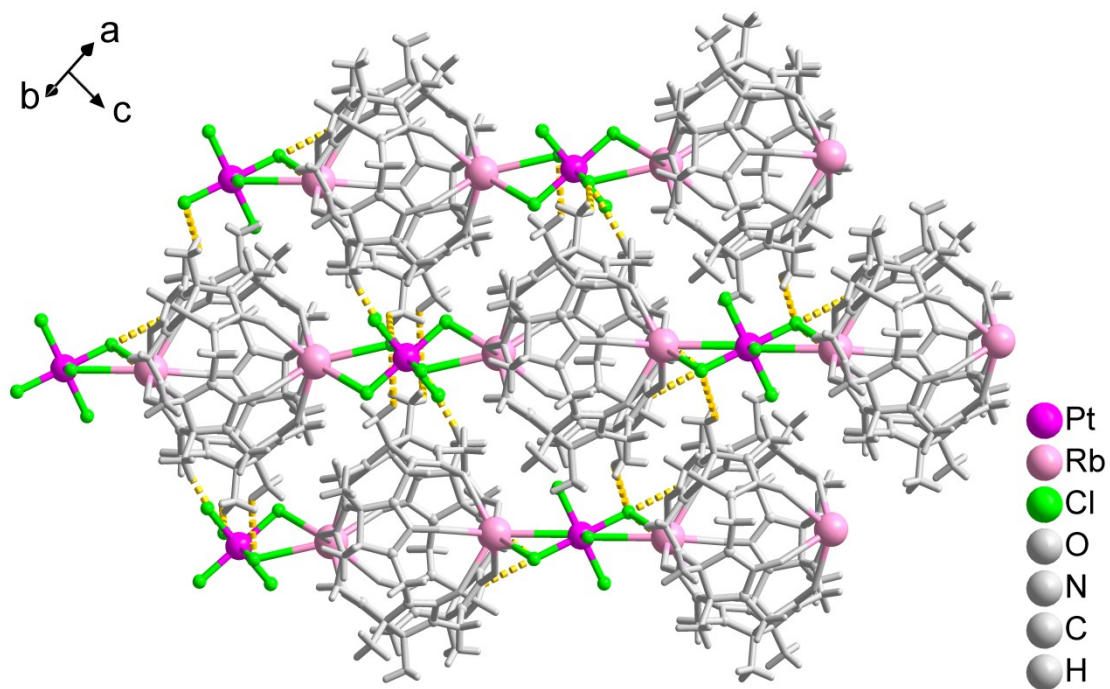


Fig. S6. The 3D images of RbPtMe₁₀CB[5].

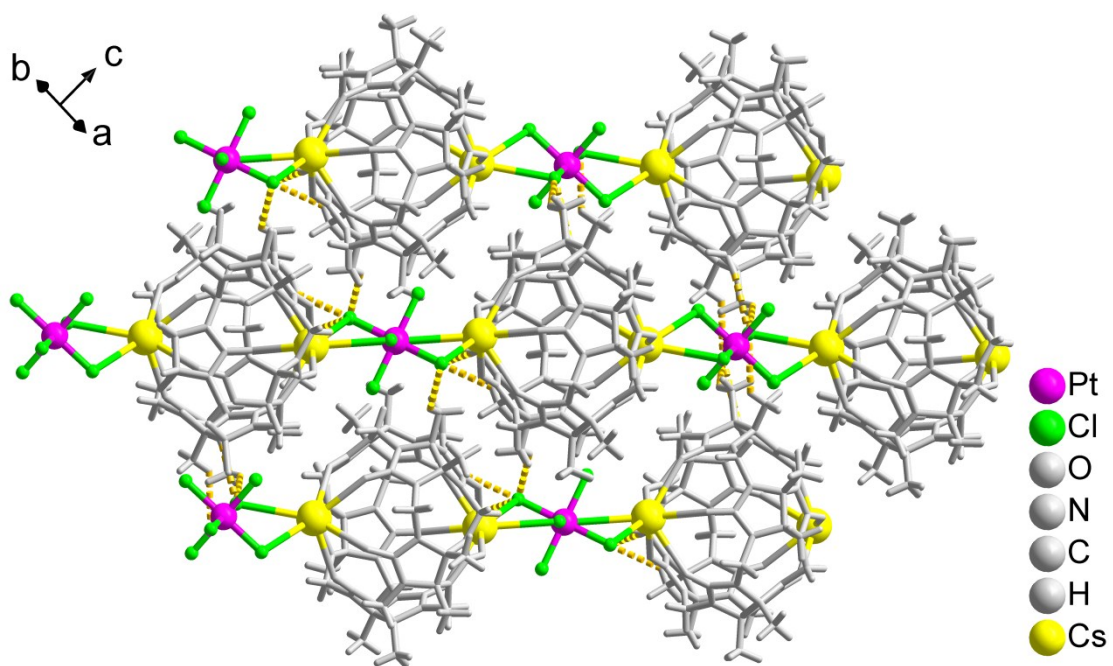


Fig. S7. The 3D images of CsPtMe₁₀CB[5].

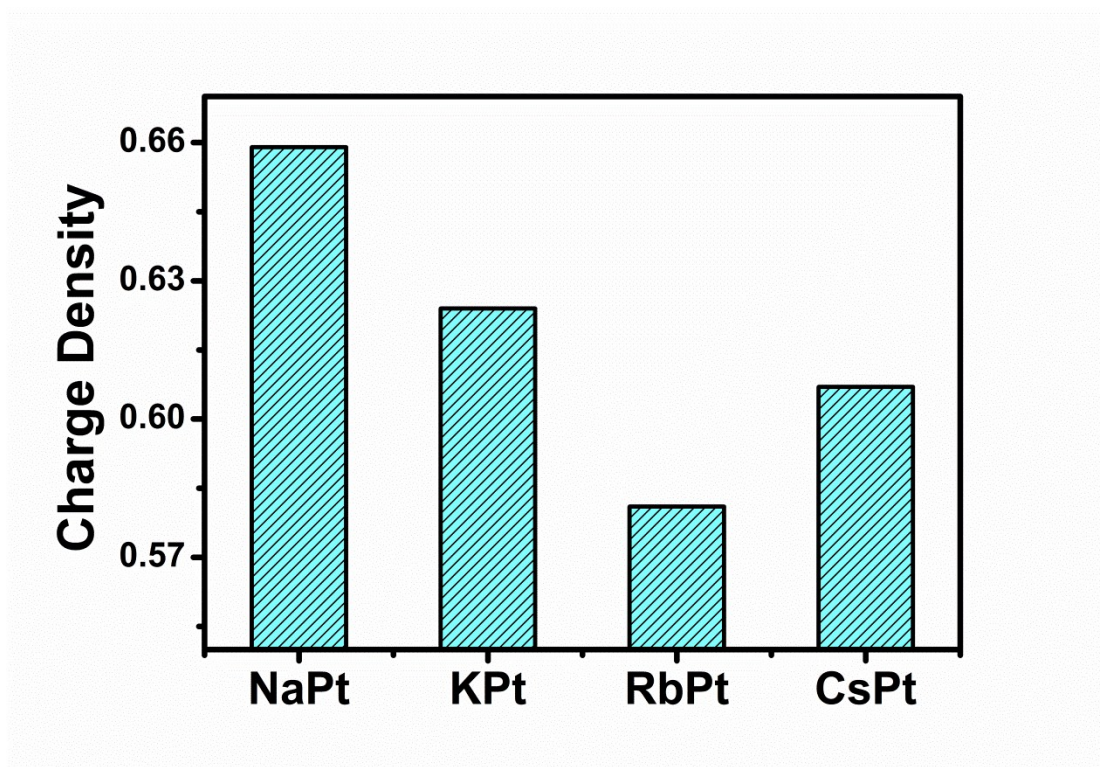


Fig. S8 Charge density of Pt atom in different complexes.

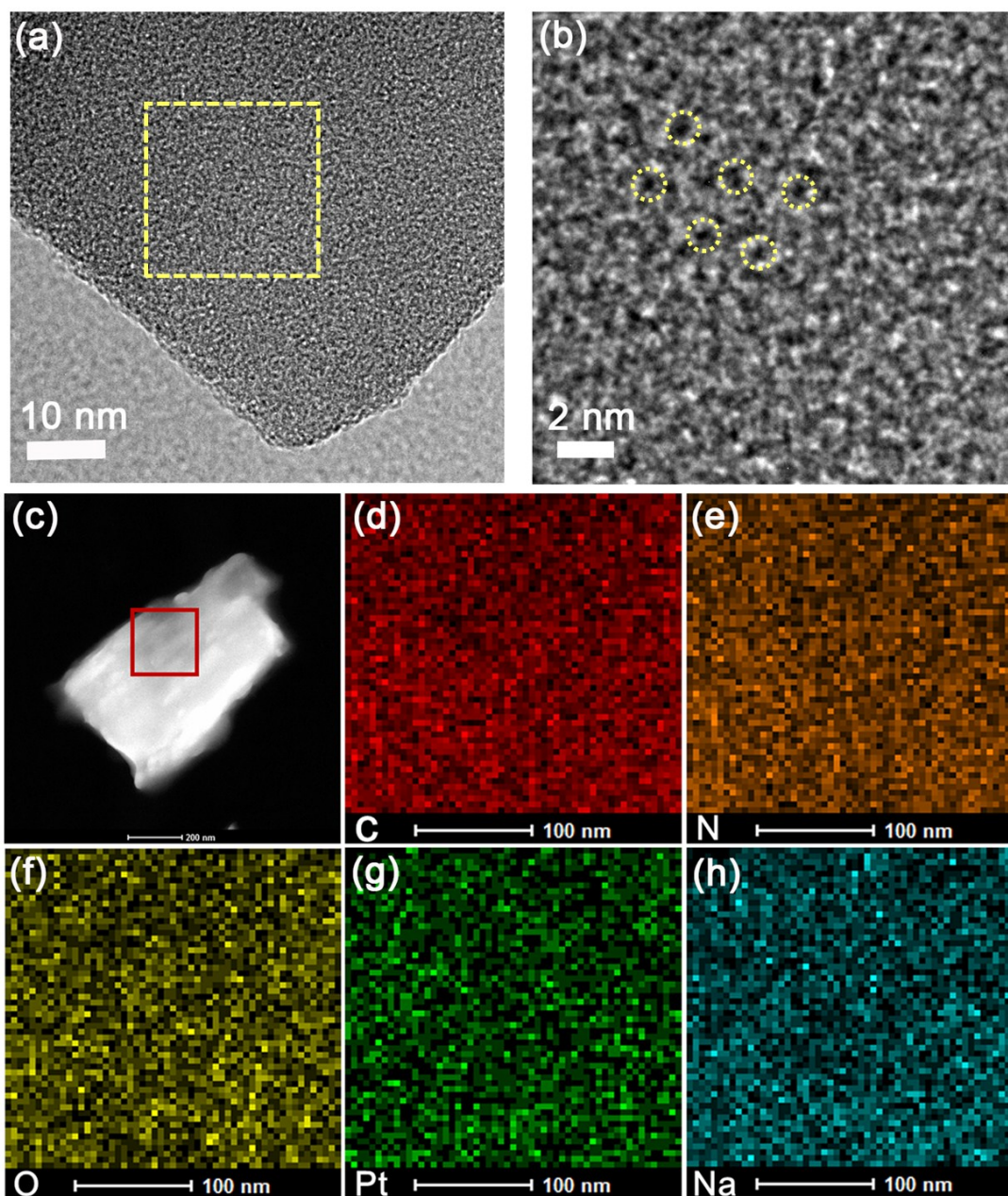


Fig. S9. (a) TEM image of NaPtMe₁₀CB[5]; (b) the IFFT pattern of the selected area. (c-h) HAADF-STEM image and the corresponding element mapping images of NaPtMe₁₀CB[5].

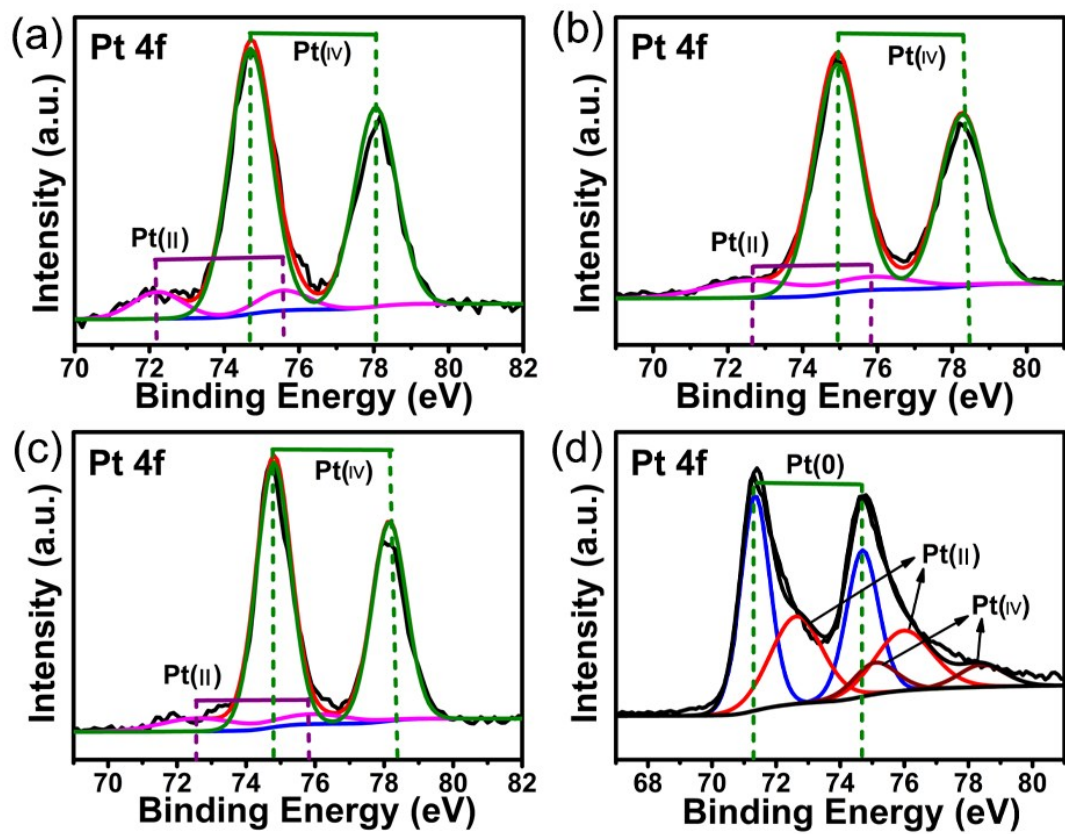


Fig. S10 XPS patterns of (a) NaPtMe₁₀CB[5] (b) KPtMe₁₀CB[5] (c) RbPtMe₁₀CB[5] (d) Pt/C.

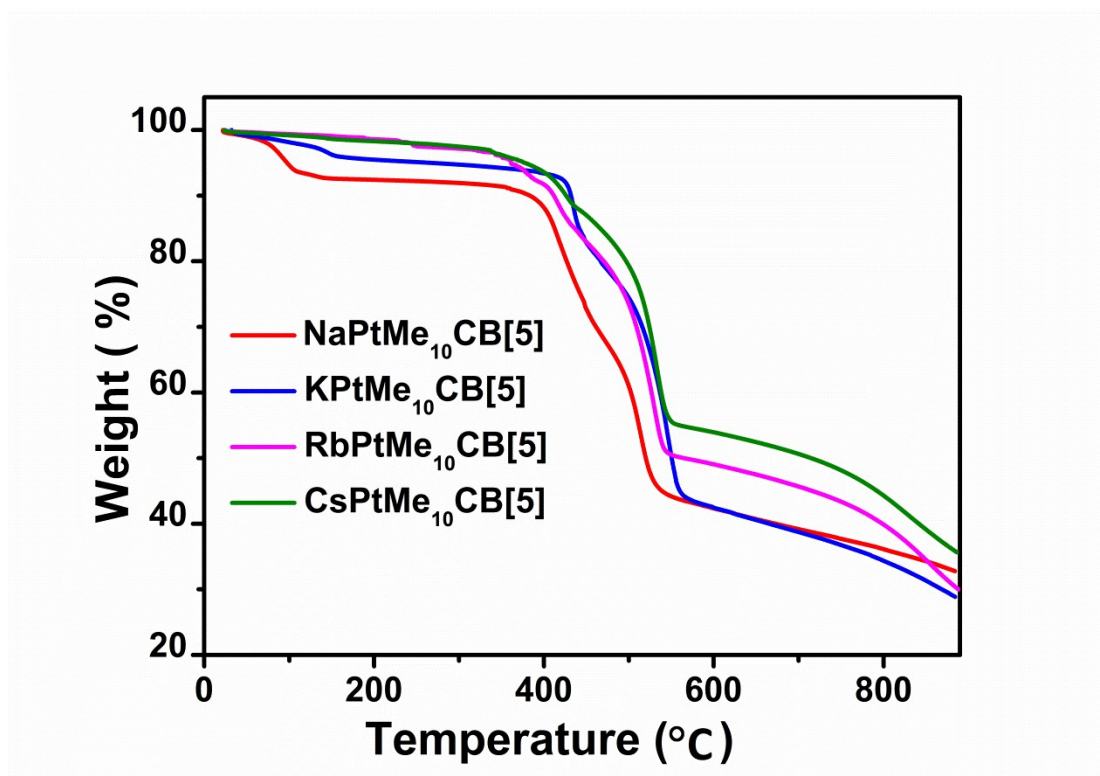


Fig. S11 TGA curves of NaPtMe₁₀CB[5], KPtMe₁₀CB[5], RbPtMe₁₀CB[5], CsPtMe₁₀CB[5].

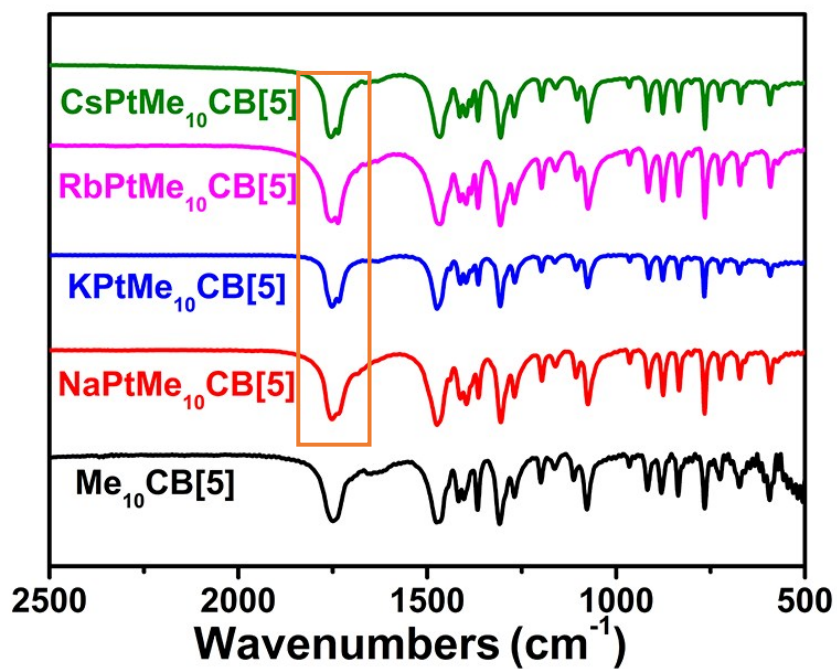


Fig. S12. IR spectra of Me₁₀CB[5], NaPtMe₁₀CB[5], KPtMe₁₀CB[5], RbPtMe₁₀CB[5] and CsPtMe₁₀CB[5].

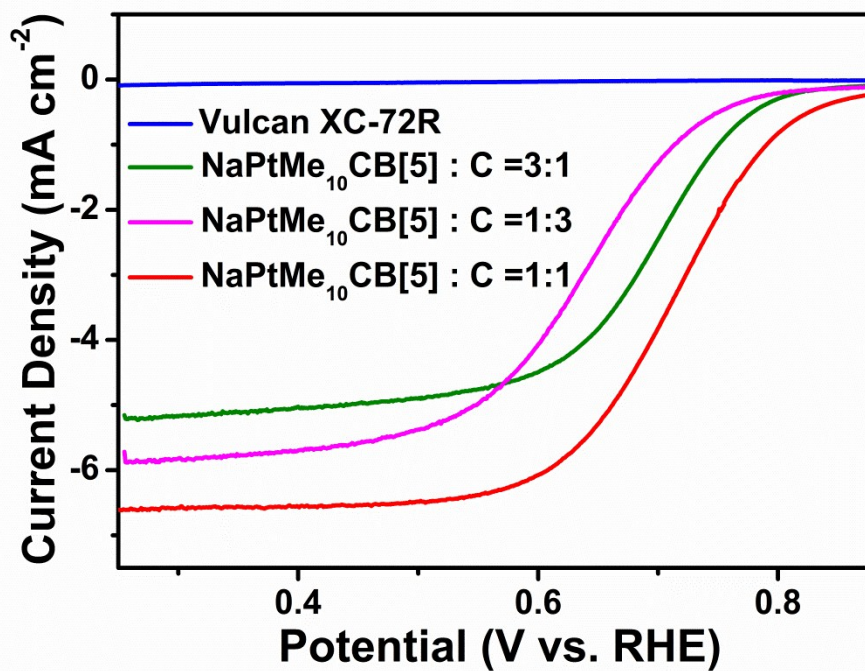


Fig. S13 LSV curves of Vulcan XC-72R, NaPtMe₁₀CB[5] at different mass ratio with Vulcan XC-72R (3:1, 1:3, 1:1).

Given the poor intrinsic electrical conductivity of supramolecular assembly, Vulcan XC-72R was introduced to mix with the as-synthesized supramolecular assembly to improve the conductivity. Taking NaPtMe₁₀CB[5] for example, the optimal mass ratio is 1:1 between NaPtMe₁₀CB[5] and Vulcan XC-72R based on the linear sweep voltammetry (LSV) curves.

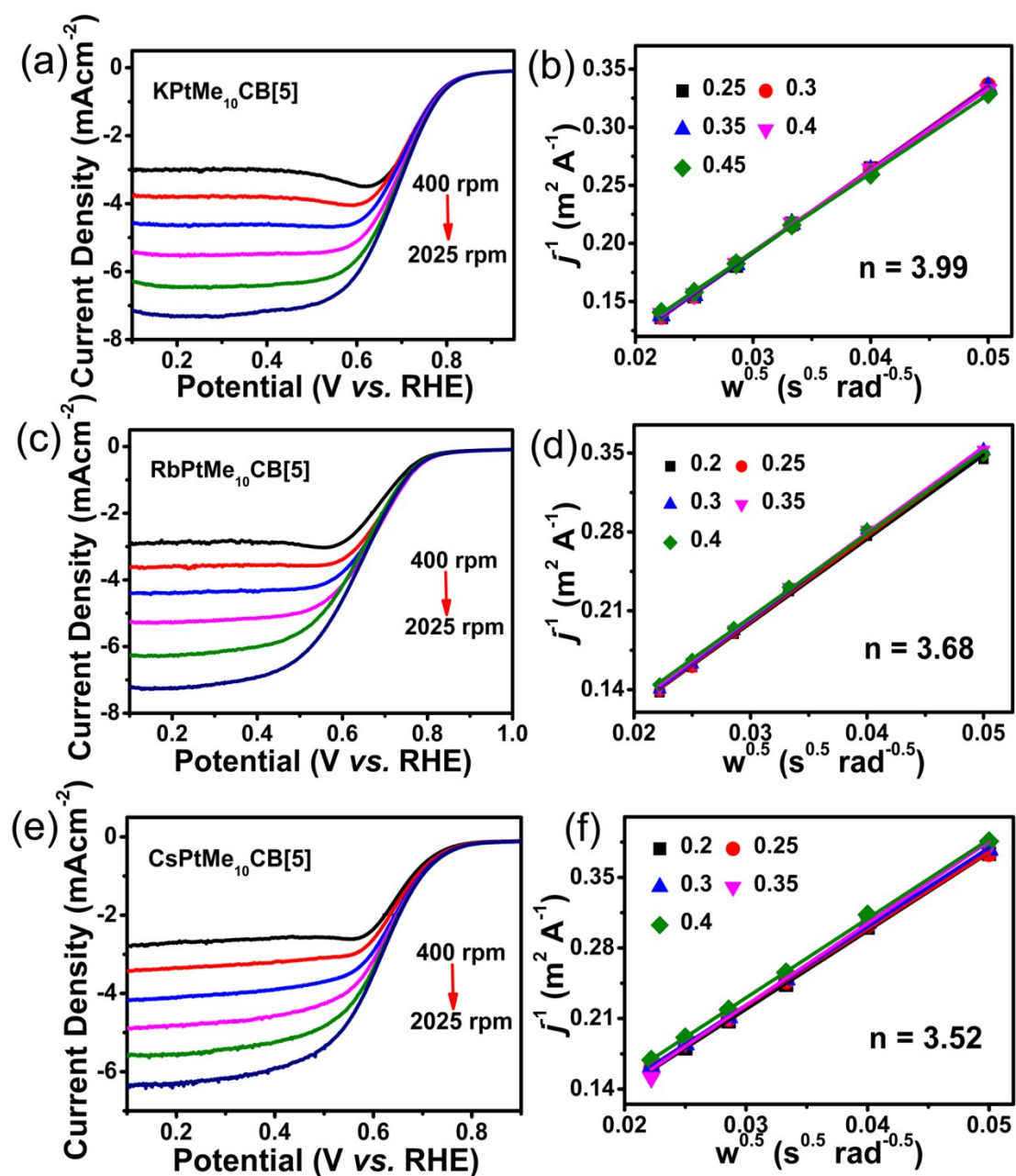


Fig. S14 Rotating disk electrode (RDE) curves of (a) KPtMe₁₀CB[5] (c) RbPtMe₁₀CB[5] (e) CsPtMe₁₀CB[5] in O₂-saturated 0.1 M HClO₄ at different speeds. The Koutecky-Levich plots of (b) KPtMe₁₀CB[5] (d) RbPtMe₁₀CB[5] (f) CsPtMe₁₀CB[5] derived from the RDE measurements.

Table S1: Crystallographic Data for the Supramolecular Assembly.

	1	2	3	4
Empirical formula	C ₄₀ H ₆₂ N ₂₀ O ₁₆ Cl ₆ Na ₂ Pt	C ₄₀ H ₅₈ N ₂₀ O ₁₄ Cl ₆ K ₂ Pt	C ₄₀ H ₅₄ N ₂₀ O ₁₂ C ₁₆ Rb ₂ Pt	C ₄₀ H ₅₄ N ₂₀ O ₁₂ C ₁₆ Cs ₂ Pt
Formula weight	1496.5	1492.5	1549	1644
Crystal System	Monoclinic			
Space group	<i>P21/m</i>	<i>P21/m</i>	<i>C2/c</i>	<i>C2/c</i>
<i>a</i> (Å)	11.0760(1)	11.0356(1)	14.7513(1)	14.8292(2)
<i>b</i> (Å)	15.1322(2)	15.2027(2)	16.6713(1)	16.6285(2)
<i>c</i> (Å)	15.9211(2)	15.7225(2)	21.8623(2)	21.9869(3)
α (°)	90	90	90	90
β (°)	92.659	93.7852	95.158	93.762
γ (°)	90	90	90	90
<i>Vol</i> (Å ³)	2665.57	2632.03	5354.68	5410.01
<i>T</i> (k)	100			
<i>Z</i>	4	4	8	8
<i>F</i> (000)	1356	1475	2920	3064
R ₁	0.0507	0.0399	0.0396	0.0272
wR ₂	0.1656	0.1207	0.1063	0.0557
GOF	1.07	1.09	1.02	1.059

Table S2: Different valence state distributions of Pt species in all the samples.

Samples	Pt	Binding Energy (eV)		Relative peak area (%)
		Pt 4f _{7/2}	Pt 4f _{5/2}	
NaPtMe ₁₀ CB[5]	Pt(II)	72.22	75.56	10.78
	Pt(IV)	74.7	78.07	89.22
KPtMe ₁₀ CB[5]	Pt(II)	72.56	75.88	12.57
	Pt(IV)	74.95	78.32	87.43
RbPtMe ₁₀ CB[5]	Pt(II)	72.58	75.82	9.4
	Pt(IV)	74.8	78.26	90.56
Pt/C	Pt(0)	71.34	74.69	51.4
	Pt(II)	72.63	75.98	37.4
	Pt(IV)	75.08	78.43	11

Table S3: ICP of Pt in all the supramolecular assemblies.

Crystals	ICP (wt %)
NaPtMe ₁₀ CB[5]	14.35
KPtMe ₁₀ CB[5]	15.34
RbPtMe ₁₀ CB[5]	14.23
CsPtMe ₁₀ CB[5]	17.34

Table S4: The comparison of the noble metal utilization efficiency.

		Pt/C	NaPtMe ₁₀ CB[5]
ECSA	m ² /g	64.9	58.26
Specific activity@0.8V	mA/cm ²	0.0494	0.01448
Mass activity@0.8V	A/mg _{Pt}	0.032	0.008438

References:

1. A. Flinn, G. C. Hough, J. F. Stoddart. and D. J. Williams, *Angew. Chem.*, 1992, **31**, 1475-1477.
2. Sheldrick, G. M. SADABS; University of Gottingen: Gottingen, Germany, 1996.
3. (a) Sheldrick, G. M. *Acta Crystallogr., Sect. A*. 1990, **46**, 467-473.; (b) Sheldrick G M. *Acta Crystallogr. C*, 2015, **71**, 3-8.
4. Frisch, M. J.; Trucks, G. W.; Schlegel, H. B., Scuseria, G. E.; Robb, M. A.; Cheeseman, J. R.; Scalmani, G.; Barone, V.; Mennucci, B.; Petersson, G. A.; Nakatsuji, H.; Caricato, M.; Li, X.; Hratchian, H. P.; Izmaylov, A. F.; Bloino, J.; Zheng, G.; Sonnenberg, J. L.; Hada, M.; Ehara, M.; Toyota, K.; Fukuda, R.; Hasegawa, J.; Ishida, M.; Nakajima, T.; Honda, Y.; Kitao, O.; Nakai, H.; Vreven, T.; Montgomery, J. A.; Jr.; Peralta, J. E.; Ogliaro, F.; Bearpark, M.; Heyd, J. J.; Brothers, E.; Kudin, K. N.; Staroverov, V. N.; Keith, T.; Kobayashi, R.; Normand, J.; Raghavachari, K.; Rendell, A.; Burant, J. C.; Iyengar, S. S.; Tomasi, J.; Cossi, M.; Rega, N.; Millam, J. M.; Klene, M.; Knox, J. E.; Cross, J. B.; Bakken, V.; Adamo, C.; Jaramillo, J.; Gomperts, R.; Stratmann, R. E.; Yazyev, O.; Austin, A. J.; Cammi, R.; Pomelli, C.; Ochterski, J. W.; Martin, R. L.; Morokuma, K.; Zakrzewski, V. G.; Voth, G. A.; Salvador, P.; Dannenberg, J. J.; Dapprich, S.; Daniels, A. D.; Farkas, O.; Foresman, J. B.; Ortiz, J. V.; Cioslowski, J.; Fox, D. J. *Gaussian 09, revision D.01*. Gaussian, Inc., Wallingford CT, 2013.
5. (a) Becke, A. D. *J. Chem. Phys.*, 1993, **98**, 5648-5652; (b) Lee, C. T.; Yang, W. T.; Parr, R. G. *Phys. Rev. B*, 1988, **37**, 785-789; (c) Grimme, S.; Antony, J.; Ehrlich, S.; Krieg, H. *J. Chem. Phys.*, 2010, **132**, 154104.
6. (a) Hay, P. J.; Wadt, W. R. *J. Chem. Phys.*, 1985, **82**, 270-283; (b) Wadt, W. R.; Hay, P. J. *J. Chem. Phys.*, 1985, **82**, 284-298; (c) Hay, P. J.; Wadt, W. R. *J. Chem. Phys.*, 1985, **82**, 299-310.
7. Lu, T.; Chen, F. W. *J. Theor. Comput. Chem.*, 2012, **11**, 163-183.
8. Lu, T.; Chen, F. W. Multiwfn: A Multifunctional Wavefunction Analyzer. *J.*

Comp. Chem., 2012, **33**, 580-592.